

Received November 12, 2019, accepted November 25, 2019, date of current version December 13, 2019.

Digital Object Identifier 10.1109/ACCESS.2019.2956568

# A Self-Adaptive and Wide-Range Conductivity Measurement Method Based on Planar Interdigital Electrode Array

XIAOLEI WANG<sup>1</sup>, YUHAO WANG<sup>2</sup>, (Senior Member, IEEE),  
HENRY LEUNG<sup>3</sup>, (Fellow, IEEE), SUBHAS CHANDRA MUKHOPADHYAY<sup>4</sup>, (Fellow, IEEE),  
SHAOPING CHEN<sup>1</sup>, AND YONGQIANG CUI<sup>1</sup>

<sup>1</sup>Hubei Key Laboratory of Intelligent Wireless Communications, South Central University for Nationalities, Wuhan 430074, China

<sup>2</sup>School of Information Engineering, Nanchang University, Nanchang 330031, China

<sup>3</sup>Department of Electrical and Computer Engineering, University of Calgary, Calgary, AB T2N 1N4, Canada

<sup>4</sup>Mechanical/Electronics Engineering, Macquarie University, Sydney, NSW 2109, Australia

Corresponding author: Yuhao Wang (wangyuhao@ncu.edu.cn)

This work was supported in part by the Hubei Provincial Natural Science Foundation of China under Grant 2018CFB377, in part by the National Natural Science Foundation of China under Grant 61801524, and in part by the Teaching and Research Foundation of South Central University for Nationalities under Grant JYX18035.

**ABSTRACT** Conductivity is a crucial parameter in water quality detection, which can roughly represent overall concentration of various inorganic ions. However, traditional conductivity sensors can only afford high performance measurement in a relatively low range while the concentration may vary much more in real-world water environment. This paper proposes a high-precision and wide-range measurement method based on a novel planar interdigital electrode sensor array and a self-adaptive algorithm. The array is composed of 3 pairs of planar electrodes with various cell constants aiming at different subdivided conductivity sections. The follow-up circuit and the self-adaptive algorithm keep the optimal electrode pair dominates the output of the array. Numerical simulations were utilized to optimize sensor parameters before fabrication. PCB manufacturing technique was used which guaranteed a relatively low manufacturing cost and stable performance. Experiments were conducted to verify the sensing performance and results showed that the array can maintain precise measurement from  $0.5\mu\text{S}/\text{cm}$  to  $500\text{ms}/\text{cm}$ .

**INDEX TERMS** Sensor arrays, environmental monitoring, conductivity, water pollution.

## I. INTRODUCTION

Conductivity is one of the most important parameters in water quality monitoring and aquatic environment protection. Since conductivity reveals amounts of inorganic ions in water [1], [2], it can act as an indicator for water pollution. For example, if conductivity measured in a lake is much higher than the standard, it may suffer from water pollution like eutrophication. Similarly, sharp changing of conductivity implies a possible pollution event. Consequently, a quick and accurate conductivity measurement is of much help in water quality monitoring that makes some water pollution detectable at its early stage, while conductivity sensor is key device for it.

The associate editor coordinating the review of this manuscript and approving it for publication was X. Huang<sup>1</sup>.

Many forms of sensors for conductivity have been proposed in different research areas. M. Asgari and K. Lee proposed a fully-integrated CMOS electrical conductivity sensor for wet media that incorporated the sensing electrodes and the readout circuitry in the same die [3]. The detection range of the sensor spanned three orders of magnitude from  $0.02\text{ mS}/\text{cm}$  to  $10\text{ mS}/\text{cm}$ . Tejaswini *et al.* designed a capacitive-coupled probe for noncontact measurement of the conductivity of liquids [4]. Lin *et al.* used microfabricated platinum electrodes for a multifunctional sensor with ability of conductivity measurement [5]. Werner and Dean introduced genetic algorithm for a better performance [6]. Adhikary *et al.* utilized phase-angle to reduce noise [7]. Wang *et al.* proposed a noncontact method for measuring the electrical conductivity of metals based on eddy current testing [8]. Xia *et al.* [9], Lambrou *et al.* [10] Cloete *et al.* [11]

developed conductivity sensor as a network node for real time monitoring of water in different fields. Sophocleous and Atkinson developed conductivity sensor for soil [12]. Liu *et al.* designed a wearable conductivity sensor for sweat monitoring [13].

However, although various types of conductivity sensor has been developed, the performance for water quality monitoring in real environment is still challenging [14]–[18]. The key problem is the balance of sensitivity and stability for wide-range measurement in a relatively harsh environment. As water conductivity in real-world scenario is unpredictable to a large extent, the measurement range should be large enough for all possible situations. But it is difficult for one sensor to maintain a reasonable sensitivity in such a wide range. Actually, it is the nature of conductivity measurement that the sensitivity will decrease as the conductivity increases for a pair of measuring electrode no matter what type of the electrode is designed. On the contrary, it is possible to maintain sensitivity to some extent if more pairs of sensing electrodes are utilized [19]. The paper proposes a novel planar sensor array with several pairs of interdigital electrodes for conductivity measurement, and a corresponding algorithm is derived to insure the sensitivity and stability in a wide conductivity ranges.

The rest of this paper is organized as follows. Section II presents a comprehensive discussion of mechanism of conductivity measurement and optimization method. Sensor design principle and parameters are discussed in section III. In Section IV, a series of experiments are conducted to verify the above theory and test the performance of the array. Section V is the conclusion and future work of this paper.

## II. MEASUREMENT PRINCIPLE AND OPTIMIZATION METHOD

### A. MEASUREMENT PRINCIPLES

Conductivity is essentially created by free mobile ions. The total conductivity  $\sigma$  depends on bulk concentration  $C$  of conducting species, their mobility  $\mu$  and charge  $z$  [20]. Obviously, there is a positive correlation between conductivity and ion concentration.

$$\sigma = z_i \mu_i C_i \tag{1}$$

Although there exist some inductive methods, conductivity is generally measured by water bulk resistance. The relationship between them was illustrated in [1], [20]. If in a bounded sample area with the surface area of the electrodes exposed to the analyzed sample  $A$ , and thickness of the sample between the electrodes  $d$ , according to Ohm's law, the bulk media resistance  $R_{BULK}$  is

$$R_{BULK} = \frac{1}{\sigma} \frac{d}{A} \tag{2}$$

It can be rewritten as

$$\sigma = \frac{1}{R_{BULK}} \frac{d}{A} = \frac{\kappa}{R_{BULK}} \tag{3}$$

where  $\kappa$  is defined as an electrode-related parameter and it is equated to  $d$  divided by  $A$  in this case.

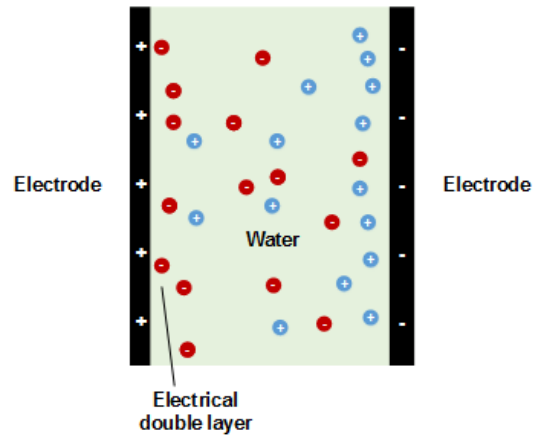


FIGURE 1. A typical measurement system for conductivity.

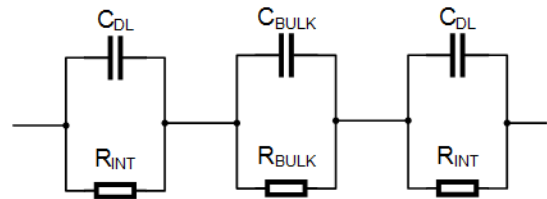


FIGURE 2. Equivalent circuit of measurement system.

Accordingly, a typical conductivity measurement system is composed of a pair of sensor electrodes and water bulk, as shown in Fig. 1. Rather than conventional resistance measurement, the water bulk has some unique characteristic. When the electrode is charged, not only water resistance will be observed but also electrical double layer (EDL) will be induced by charges of different polarity at the interface. EDL usually forms an imperfect capacitance which can be seen as a parallel connection of EDL capacitor and an interface resistance.

Correspondingly, equivalent circuit of the measurement system can be established as shown in Fig. 2. Besides of the parallel connection of water bulk resistance  $R_{BULK}$  and water bulk capacitance  $C_{BULK}$ , there exist interfacial impedances composed of EDL capacitor  $C_{DL}$  and interface resistance  $R_{INT}$ . Theoretically,  $R_{BULK}$  can be directly calculated based on the circuit, but a better approach is elimination of capacitive part by frequency selection. Usually, EDL may mostly diminish when applied AC frequency is above 1000 Hz, as there is not enough time for ion accumulation at a higher frequency. For the parallel connection of  $R_{BULK}$  and  $C_{BULK}$ , it would be resistive when frequency is low, and it will become capacitive if frequency is high enough. For common water which is not highly purified,  $C_{BULK}$  is mostly observed at megahertz range. So the total impedance can be simplified as a pure resistance at some certain frequency ranges between 1K Hz and 1M Hz.

Nonetheless, water conductivity is more than a mere resistance measurement in real-world aquatic environment.

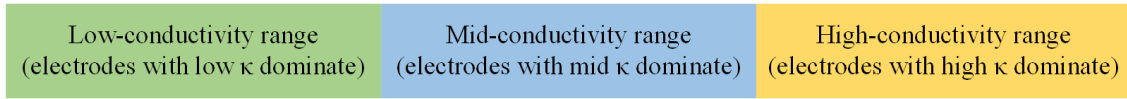


FIGURE 3. Subdivision of conductivity range and corresponding  $\kappa$ .

The problem is to maintain performance in a wide conductivity range. As a key performance indicator, sensitivity can be calculated as

$$S = \frac{dR}{d\sigma} = \frac{d\frac{\kappa}{\sigma}}{d\sigma} = -\frac{\kappa}{\sigma^2} \quad (4)$$

Equation (4) implies the sensitivity will inevitably drop as conductivity increases no matter what cell constant is designed. Apparently, a bigger  $\kappa$  is needed for a relative high sensitivity, but a mere giant  $\kappa$  alone is not enough because it leads to less stability. According to (3),  $\kappa$  acts as an amplification factor between  $\sigma$  and  $1/R$ , so every measuring error will be multiplied by  $\kappa$ . Meanwhile, a bigger  $\kappa$  also means a greater range of resistance variation, so it challenges subsequent circuit in measurement accuracy and bring more quantization noise. Moreover, adding of  $\kappa$  will increase difficulty in sensor fabrication to some extent. Taking parallel-plate electrodes for example, augment of  $\kappa$  means increasing the distance between the electrodes and decreasing the area which not only make the sensor greater in size but also unstable in the measurement. In conclusion, a high  $\kappa$  is preferred in high-conductivity water environment for its sensitivity, but a relatively small  $\kappa$  may have a better overall performance in low-conductivity environment.

## B. SELF-ADAPTIVE ALGORITHM

It is clear that only one measuring electrode alone, regardless of what  $\kappa$  is set, can not afford high performance measurement in a wide concentration range. However, a sensor array may make it possible. The array can be composed of several pairs measuring electrodes which are with different  $\kappa$  aiming at various subdivided concentration ranges. As each pair dominates various concentration ranges where they can keep reasonable sensitivities, it is possible to maintain both sensitivity and stability.

Suppose the whole conductivity scope is divided into 3 parts which are low-conductivity range, mid-conductivity range and high-conductivity range. Then 3 central conductivity  $C_c$  can be introduced to represent each subdivide range, which is defined as

$$C_c = \sqrt{C_{\max}C_{\min}} \quad (5)$$

where  $C_{\max}$  is the max conductivity in subdivided range while  $C_{\min}$  is the minimum.

Then, a sensor array composed of 3 pairs of measuring electrodes with different  $\kappa$  can be designed aiming at corresponding subdivided conductivity ranges. To be specific, electrodes with the smallest cell constant  $\kappa$  should dominate the measurement in low-conductivity range, and electrodes with a bigger  $\kappa$  for mid-conductivity range while the biggest

$\kappa$  for high-conductivity range. As shown in Fig. 3, each electrode pair have a preferred subdivided conductivity range in which the electrodes may have their best measuring performance. Since 3 measurement results would be obtained by 3 pairs of electrodes, the final conductivity can be demonstrated as

$$\sigma_{final} = \frac{\beta_1\sigma_1 + \beta_2\sigma_2 + \beta_3\sigma_3}{\beta_1 + \beta_2 + \beta_3} \quad (6)$$

where  $\beta$  is the weight coefficient for each measurement. Apparently, a bigger  $\beta$  makes corresponding measurement more dominative in the final result. It is also obvious that the sensitivity of the combination measurement can be represented as

$$S_{final} = \frac{\beta_1S_1 + \beta_2S_2 + \beta_3S_3}{\beta_1 + \beta_2 + \beta_3} \quad (7)$$

For a self-adaptive method, all  $\beta$  should automatically change with current conductivity measured, so that the optimal electrode can always have the biggest  $\beta$ . Since each electrode targets at a subdivided range with a unique central conductivity  $C_c$ , if the measurement result is closed to a certain  $C_c$ , corresponding electrodes deserve a huge  $\kappa$ . The nearer measurement of an electrode approximates to its corresponding central conductivity, a bigger  $\beta$  it should have. Then,  $\beta$  is defined as

$$\beta = \left(\frac{\sigma}{C_c} + \frac{C_c}{\sigma}\right)^{-1} \quad (8)$$

where  $\sigma$  is measurement result from a pair of electrode and  $C_c$  is its targeted conductivity. For each pair of measurement electrodes, relationship between  $\beta$ ,  $\sigma$  and  $C_c$  is shown in Fig. 4. Obviously, for any electrodes, the maximum value of  $\beta$  can be achieved when measured conductivity  $\sigma$  is equated to its matching  $C_c$ . The more conductivity is deviated from its corresponding  $C_c$ , the smaller  $\beta$  is obtained. Except for extreme case that measured conductivity is equated to a boundary value between two subdivision, the conductivity would inevitably fall into one conductivity subdivided zone where the relevant electrodes certainly have a bigger  $\beta$ . And it is all right for two pairs of electrodes share the same  $\beta$  at a boundary conductivity. Thus the setting of  $\kappa$  can ensure that the optimal electrodes will always be dominative when measured conductivity is closed to its corresponding  $C_c$ .

Furthermore, the process of auto optimization for  $\beta$  can be achieved and simplified by measurement circuit and reference resistor setting. The electrical equivalent circuit of measurement is shown in Fig. 5. The sensor is connected to an AC supply, and  $R_r$  denotes the reference resistor connected to the sensor.  $V_1$  can be seen as input from AC supply while  $V_2$  is voltage on  $R_r$ .

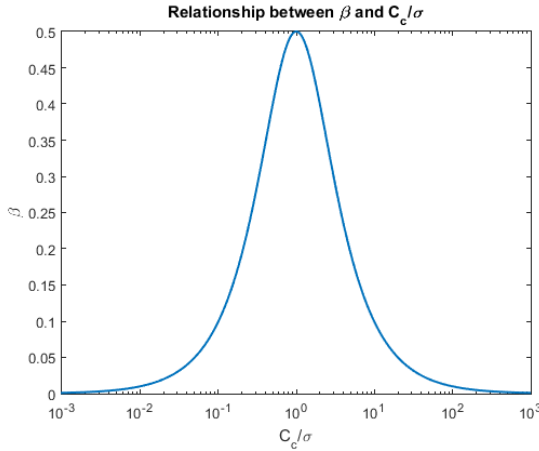


FIGURE 4. Relationship between  $\beta$  and  $C_c/\sigma$ .

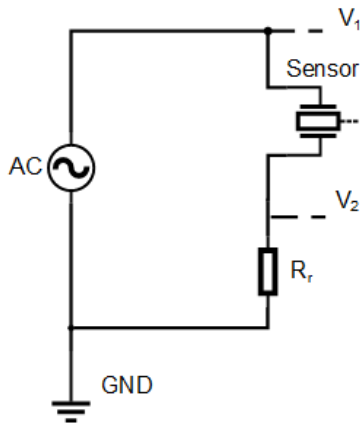


FIGURE 5. Electrical equivalent circuit of the measurement.

When the EDL effect and other capacitive effect are greatly reduced by frequency selection, the impedance of the sensor is purely resistive and can be expressed as

$$R_s = R_{BULK} = \frac{V_1}{V_2} R_r - R_r = \frac{V_1 - V_2}{V_2} R_r \quad (9)$$

So it is easy to calculate  $R_s$  from the measurement as well as corresponding  $\sigma$ , because  $R_{BULK}$  is equated to  $\kappa/\sigma$ . Obviously,  $R_s$  is alterable as it depends on concentration of ions in water, while  $R_r$  is a fixed parameter in the circuit which is set as

$$R_r = \frac{\kappa}{C_c} \quad (10)$$

where  $\kappa$  is the cell constant of the electrodes, and  $C_c$  is its corresponding central conductivity.

Therefore, each measurement circuit may have a certain  $R_r$  which is calculable. With definition of  $R_r$ , calculation for  $\beta$  can be transformed as

$$\begin{aligned} \beta &= \left( \frac{\sigma}{C_c} + \frac{C_c}{\sigma} \right)^{-1} = \left( \frac{\kappa/\sigma}{\kappa/C_c} + \frac{\kappa/C_c}{\kappa/\sigma} \right)^{-1} \\ &= \left( \frac{R_s}{R_r} + \frac{R_r}{R_s} \right)^{-1} = \left( \frac{V_1 - V_2}{V_2} + \frac{V_2}{V_1 - V_2} \right)^{-1} \quad (11) \end{aligned}$$

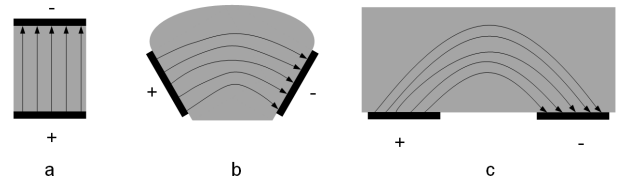


FIGURE 6. Transformation from parallel-plate electrode to planar electrode.

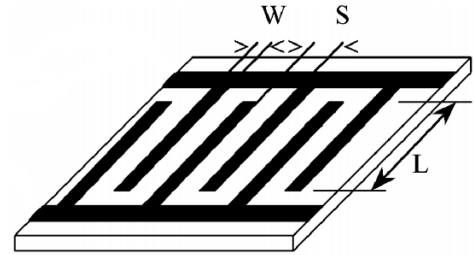


FIGURE 7. Basic structure of planar electrode.

Then,  $\beta$  can be easily calculated with two voltage measurements and a well-designed  $R_r$ . Moreover, self-adaptive optimization for conductivity can be also achieved. Through the whole measurement and calculation,  $\kappa$  setting plays a critical role as it not only equilibrates overall sensing performance in different subdivided range, but also has direct relationship with  $R_r$  and  $R_s$ . Instead of direct assignment, value of  $\kappa$  comes from structure of electrodes which is related to all geometric parameters.

### III. SENSOR DESIGN AND FABRICATION

#### A. PLANAR ELECTRODE SENSOR

Traditional parallel-plate electrode is not eligible for the array because of its space construction. Planar structure, on the contrary, can integrate electrode pairs with various cell constants in a single board which not only provide a stable structure but also reduce overall cost.

As shown in Fig. 6, planar electrode can be seen as the transform of parallel-plate electrode. Rather than stereo structure of parallel plate, planar electrode can be seen as a 2D structure with more stability and flexibility. A typical structure of planar electrode can be seen in Fig. 7. The major structural parameters are electrode length  $L$ , electrode number  $N$ , electrode width  $w$ , and electrode space  $s$ . Due to one-side access structure, it is much more flexible than parallel-plate structure. The cell constant  $\kappa$  is designable by fingers config as

$$\kappa = \frac{\epsilon_0 \epsilon_r}{C} = \frac{1}{(N-1)L} \frac{2K(k)}{K[(1-k^2)^{1/2}]} \quad (12)$$

where  $K(k)$  is the complete elliptic integral of the first kind:

$$K(k) = \int_{t=0}^1 \frac{dt}{[(1-t^2)(1-k^2t^2)]^{1/2}} \quad (13)$$

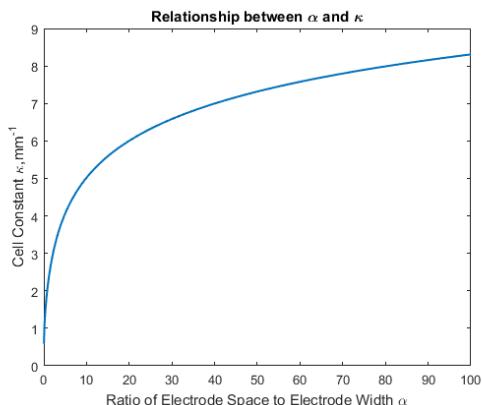


FIGURE 8. Influence of electrode space and electrode width.

$k$  is related to geometric parameters. When there is only two fingers,  $k$  can be approximated by

$$k = \frac{s}{s + w} \tag{14}$$

When  $N$  is more than two fingers,  $k$  is defined as

$$k = \cos\left(\frac{\pi}{2} \frac{w}{s + w}\right) \tag{15}$$

For simplifying equations,  $\alpha$  is introduced which is defined as the ratio of electrode space  $s$  and electrode width  $w$

$$\alpha = \frac{s}{w} \tag{16}$$

Then both (14) and (15) can be reduced, and (12) can be rewritten as following when fingers are more than two

$$\kappa = \frac{\epsilon_0 \epsilon_r}{C} = \frac{1}{(N - 1)L} \frac{2K \left[ \cos\left(\frac{\pi}{2} \frac{1}{\alpha + 1}\right) \right]}{K \left[ \sin\left(\frac{\pi}{2} \frac{1}{\alpha + 1}\right) \right]} \tag{17}$$

Accordingly,  $\kappa$  can be calculated precisely by parameter setting. As discussed above, a higher  $\kappa$  should be utilized in water environment with higher conductivity for a proper sensitivity. Thus, after potential conductivity range in real-world water environment being divided into several parts, an array with a series of  $\kappa$  can be accordingly designed, so that each pair of electrodes can deal with a subdivided conductivity range, keeping the both sensitivity and stability. The specific parameters can be obtained by simulation and then be utilized in the fabrication.

**B. SIMULATION**

Matlab is employed for numerical simulation to reveal relationship between geometric parameters and  $\kappa$  based on (17). The relationship between  $\alpha$  and  $\kappa$  is analyzed and shown in Fig. 8, where  $N$  is set as 10 and  $L$  is 0.1 mm. Distinctly, there is a sharp augment of  $\kappa$  as  $\alpha$  increases when it is very small, and the trend slows down as  $\alpha$  grows. It is also inferred that increasing  $s$  or decreasing  $w$  may enhance  $\kappa$ , and vice versa.

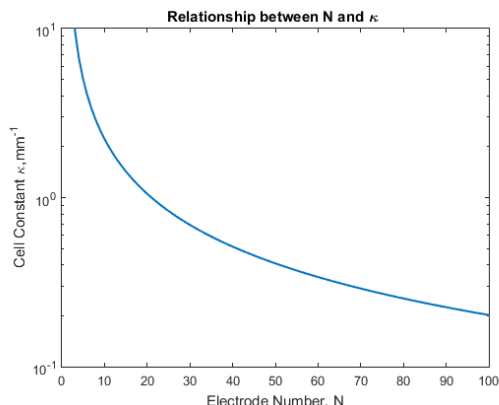


FIGURE 9. Influence of electrode number.

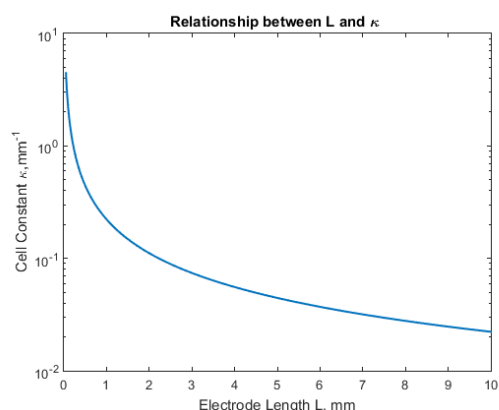


FIGURE 10. Influence of electrode length.

TABLE 1. Geometrical parameters and simulation results.

Group	Space	Width	Number	Length	$\kappa$ (calculated by Matlab)
1	10mm	1mm	4	5mm	0.30mm <sup>-1</sup>
2	4mm	2mm	10	10mm	0.029mm <sup>-1</sup>
3	1mm	5mm	20	20mm	0.0029mm <sup>-1</sup>

Effect of electrode number  $N$  is shown in Fig. 9, where  $\alpha$  is set as 1 and  $L$  is set as 0.1 mm. Fig. 10 reveals the effect of  $L$  where  $N$  is set as 10 and  $\alpha$  is set as 1. Both effects of  $N$  and  $L$  are similar and increasing of each will reduce  $\kappa$ . It is also noticeable that  $N$  should be an integer while  $L$  is much more customizable. If both  $N$  and  $L$  alter with the same trend,  $\kappa$  will change remarkably.

After effects of geometrical parameter has been revealed, some specific parameters for  $\kappa$  were set and simulation results were shown in table 1. With three groups of parameters, three  $\kappa$  were figured out. Basically,  $\kappa_1$  is 10 times  $\kappa_2$ , and  $\kappa_2$  is 10 times  $\kappa_3$ . Simulation results suggested that the adjusting of electrode parameters can designedly change  $\kappa$ , and the parameters were used for sensor fabrication.

**C. SENSOR FABRICATION**

Sensor array was fabricated using printed circuit board technology which was with advantage of rapid manufacturing,

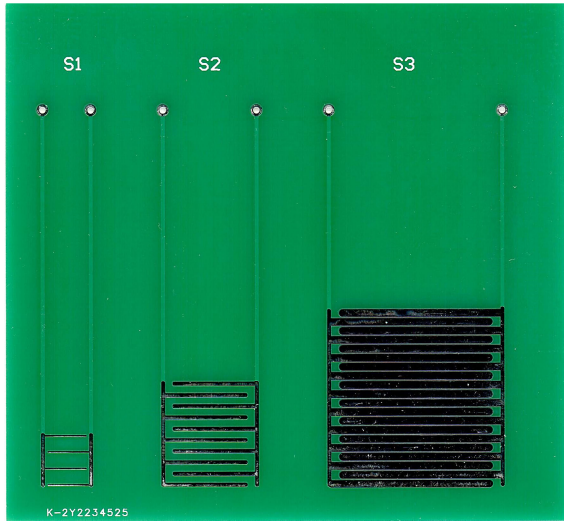


FIGURE 11. Sensor array.

low cost and stable property. The array was composed of 3 pairs of sensing electrodes, and related parameters were the same as in Table 1.

Fig. 11 shows fabricated sensor array. The base board was made of FR-4 glass-reinforced epoxy laminate material, and the whole board size was  $75\text{ mm} * 70\text{ mm} * 1.6\text{ mm}$ . The three pairs were marked as S1, S2 and S3. Only sensing part was exposed and some pads were designed for lead wire. Stannum was used to cover sensing copper electrode for protection, and the thickness of copper and stannum were  $35\text{ }\mu\text{m}$  and  $20\text{ }\mu\text{m}$ .

#### IV. EXPERIMENTS

##### A. MEASUREMENT SETTING

Basic principle of measurement follows the idea in Fig. 5 and the real experiment setting is represented in Fig. 12. A Siglent SOG2122X function waveform generator was used to create standard sinusoidal waveform with peak-to-peak value of 5 V and frequency of 10 kHz as input. A Tektronix MOD3104 mixed domain oscilloscope was used to record the both input and output. The three pairs shared the same input as V1 and had 3 different outputs as V2. A beaker was used for the sample container and the sensing part was totally immersed into the water sample. All the experiments were conducted at 25 degrees Celsius.

##### B. CALIBRATION OF CELL CONSTANT

The first step was calibration of  $\kappa$  with two commercial conductivity sensors from Suntex and Sinomeasure. A group of water samples were carefully prepared with the conductivities of  $5\text{ }\mu\text{S/cm}$ ,  $10\text{ }\mu\text{S/cm}$ ,  $20\text{ }\mu\text{S/cm}$ ,  $50\text{ }\mu\text{S/cm}$ ,  $100\text{ }\mu\text{S/cm}$ ,  $200\text{ }\mu\text{S/cm}$ ,  $500\text{ }\mu\text{S/cm}$ ,  $1\text{ mS/cm}$ ,  $2\text{ mS/cm}$ ,  $5\text{ mS/cm}$ ,  $10\text{ mS/cm}$ ,  $20\text{ mS/cm}$ , and  $50\text{ mS/cm}$ . The conductivity range can cover most cases which may happen in reality from pure water to concentrated liquor. Another purpose for the test is checking whether the capacitive impedance is reduced. Measurement results

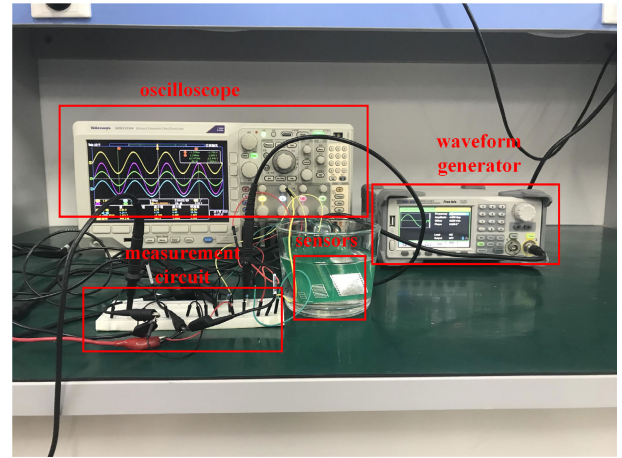


FIGURE 12. Experiment setting.

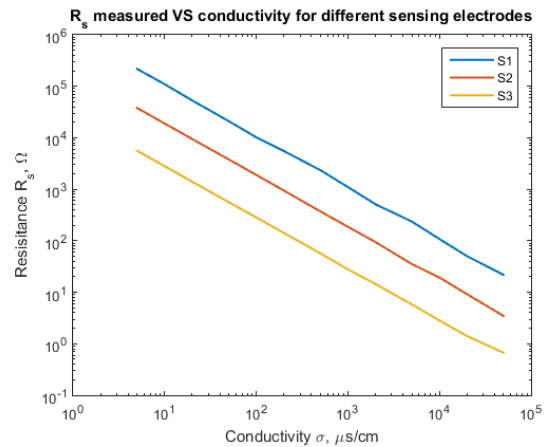


FIGURE 13.  $R_s$  measured at different Conductivities.

from different samples showed that there were little phase differences between  $V_1$  and  $V_2$  in each case implying the capacitive part of impedance was eliminated. Fig.13 showed the relationship between conductivity and  $R_s$  measured.

Distinctly, all three electrodes showed nearly perfect reciprocal relationship between conductivity and resistance. Then, three  $\kappa$  were calculated as  $0.11\text{ mm}^{-1}$  for S1,  $0.021\text{ mm}^{-1}$  for S2, and  $0.0028\text{ mm}^{-1}$  for S3. Compared to simulation result in table 1, sensor 3 showed highly consistency, but  $\kappa$  of sensor 2 and sensor 1 were smaller than those from simulation. Reasons for the deviation may be that simulation of Matlab only considered one side of corresponding electrodes in 2D model while the sensor array was a 3D device in reality. Taking the height of electrodes into consideration, the electrodes should be more conductive than those from mere numerical simulation, especially when the electrode number is very small. So the  $\kappa$  from simulation were smaller than those from experiments. With growing of electrode number, the effect of electrode height was weakened, and experiment was closed to simulation result.

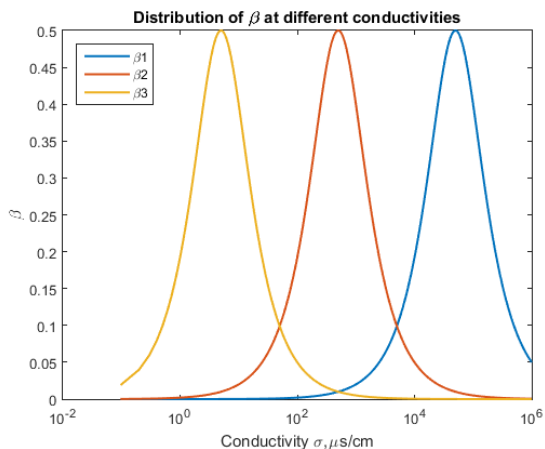


FIGURE 14. Distribution of  $\beta$  at different conductivities.

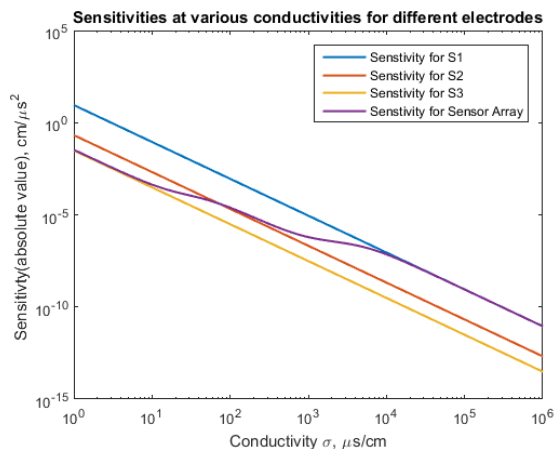


FIGURE 15. Sensitivities of different electrodes at various conductivities.

**C. WEIGHT COEFFICIENT AND SENSITIVITY**

After calculation of  $\kappa$ , 3 central conductivities were required. The total measurement range was set from  $0.5\mu\text{s/cm}$  to  $500\text{ms/cm}$  which was wide enough for water environment detection. The range was then divided into 3 groups:  $0.5\mu\text{s/cm}$  to  $50\mu\text{s/cm}$ ,  $50\mu\text{s/cm}$  to  $5\text{ms/cm}$ , and  $5\text{ms/cm}$  to  $500\text{ms/cm}$ , forming 3 central conductivities  $5\mu\text{s/cm}$ ,  $500\mu\text{s/cm}$ , and  $50\text{ms/cm}$ . Thus, three  $R_r$  can be calculated as  $22\Omega$ ,  $380\Omega$ , and  $5600\Omega$ . Since both central conductivities  $C_c$  and reference resistances  $R_r$  had been confirmed, distribution of each weight coefficient  $\beta$  in the whole measurement range can be calculated.

The changing of each  $\beta$  with various conductivities was shown in Fig. 14. As conductivity grows, sensor 3 dominates the lowest conductivity range with  $\beta_3$ , sensor 2 dominates mid conductivity range with  $\beta_2$ , and sensor 1 dominates the highest conductivity range with  $\beta_1$ . The variation tendency of  $\beta$  is desirable as sensor 3 has the minimum  $\kappa$ , sensor 2 has medium  $\kappa$  and sensor 1 had the highest  $\kappa$ .

Sensitivity variations were according calculated too. As shown in Fig. 15, sensitivities for  $S_1$ ,  $S_2$ , and  $S_3$  were calculated according to (4), while the final sensitivity of the array was calculated on basis of (7) and data of  $\beta$  in Fig. 15. Each sensitivity dropped as conductivity increased, but the compositive sensitivity from the array had a better performance than any single sensing pair. It kept a relatively small value in low conductivity range, and a relatively high value in high conductivity zone which was an optimal working strategy for overall sensing performance as discussed before.

**D. REPRODUCIBILITY AND MEASUREMENT RANGE ANALYSIS**

More tests were conducted for stability and reproducibility. Seven samples were prepared for the array and commercial sensors. Sample 3, sample 4, and sample 5 had similar conductivity, while other samples have various conductivities. Thus both reproducibility and overall detection performance can be evaluated.

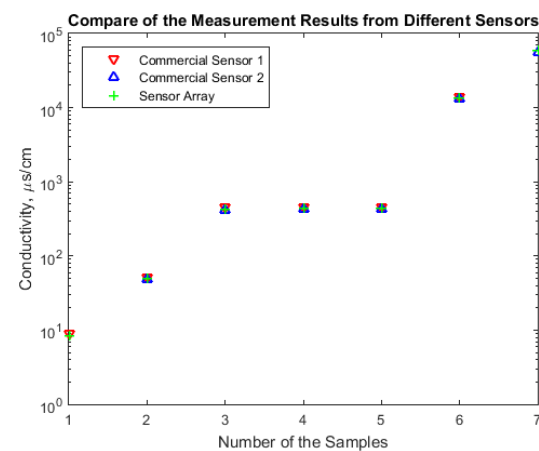


FIGURE 16. Measurement results from different sensors at various conductivities.

As represented in Fig. 16, results showed that the array had equivalent sensing performance compared to commercial sensors. Comparison from sample 3, 4, and 5 verified the reproducibility of the array, as they showed high consistency. It was also observed that the array had a wider measurement range than two commercial sensors, since sample 1 was beyond measurement range of commercial sensor 2 while sample 7 was out of the measurement range of commercial sensor 1. The wide range measurement may be attributed to dynamic  $\kappa$ . It is clear that a large  $\kappa$  results in a huge resistance, especially in a low conductivity environment. Similarly, a small resistance will be observed in high conductivity environment with a tiny  $\kappa$ . Thus, the two extremum values limited both measuring precision and measuring range. The bigger gap between them, the more difficult it is for the measurement. But the overall measuring performance can be greatly improved by compositive measurement of the array. Table 2 shows extremum resistance values and corresponding  $\beta$  measured in experiments.

Apparently,  $2.2\text{M}\Omega$  was maximum resistance value while  $0.056\Omega$  was the minimum, and either of them challenged

**TABLE 2. Extremum values and corresponding  $\beta$ .**

Group	$R_{max}(0.5\mu s/cm)$	$\beta(R_{max})$	$R_{min}(500ms/cm)$	$\beta(R_{min})$
S1	2.2M $\Omega$	$9.9 * 10^{-6}$	2.2 $\Omega$	$9.9 * 10^{-2}$
S2	0.42M $\Omega$	$9.9 * 10^{-4}$	0.42 $\Omega$	$9.9 * 10^{-4}$
S3	0.056M $\Omega$	$9.9 * 10^{-2}$	0.056 $\Omega$	$9.9 * 10^{-6}$

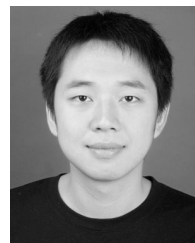
the measurement. However, as the two extreme values have very tiny  $\beta$ , they were much less important than other values in the final result of the sensing array. Actually, 0.056M $\Omega$  rather than 2.2M $\Omega$ , and 2.2 $\Omega$  rather than 0.056 $\Omega$  dominated the measurement as the maxima and minima. Therefore, the maximum resistance needed in reality was reduced by 97% while the minimum resistance needed is increased by 39 times, which greatly lower the requirement of subsequent circuit. Consequently, both conductivity range and measurement accuracy can be enhanced.

## V. CONCLUSION

This paper proposes a high-precision and wide-range conductivity method based on novel planar electrode sensor array and a self-adaptive algorithm. A planar electrode array with 3 different pairs of sensing electrodes were simulated and fabricated, and each pair had a various cell constant. Taking advantages of weight coefficient and central conductivity, the algorithm guaranteed that the optimal sensing electrodes always dominated measurement result. And the setting of follow-up circuit made the calculation easy. The array was calibrated with commercial conductivity sensors and tested in different water samples. Result analysis showed that the array kept a reasonable sensitivity, good reproducibility and a wider measurement range. More sensors with different electrode parameters will be fabricated by microelectronics technology in future, and an embedded system with idea of IoT will be applied.

## REFERENCES

- [1] X. Wang, Y. Wang, H. Leung, S. C. Mukhopadhyay, M. Tian, and J. Zhou, "Mechanism and experiment of planar electrode sensors in water pollutant measurement," *IEEE Trans. Instrum. Meas.*, vol. 64, no. 2, pp. 516–523, Feb. 2015.
- [2] X. Wang, Y. Wang, H. Leung, S. Mukhopadhyay, M. Tian, and J. Zhou, "Inorganic material detection based on electrode sensor," *IEEE Sensors J.*, vol. 16, no. 11, pp. 4147–4148, Jun. 2016.
- [3] M. Asgari and K.-S. Lee, "Fully-integrated CMOS electrical conductivity sensor for wet media," *IEEE Sensors J.*, vol. 19, no. 15, pp. 6445–6451, Aug. 2019.
- [4] K. K. Tejaswini, B. George, V. J. Kumar, R. Srinivasan, and T. Sudhakar, "A capacitive-coupled noncontact probe for the measurement of conductivity of liquids," *IEEE Trans. Instrum. Meas.*, vol. 68, no. 5, pp. 1602–1610, May 2019.
- [5] W.-C. Lin, K. Brondum, C. W. Monroe, and M. A. Burns, "Multifunctional Water Sensors for pH, ORP, and conductivity using only microfabricated platinum electrodes," *Sensors*, vol. 17, p. 1655, Jul. 2017.
- [6] F. T. Werner and R. N. Dean, "Characterising a PCB electrical conductivity sensor using electromagnetic simulation and a genetic algorithm," *IET Sci., Meas. Technol.*, vol. 11, no. 6, pp. 761–765, Sep. 2017.
- [7] A. Adhikary, G. Kumar, S. Banerjee, S. Sen, and K. Biswas, "Modelling and performance improvement of phase-angle-based conductivity sensor," in *Proc. IEEE 1st Int. Conf. Control, Meas. Instrum. (CMI)*, Kolkata, India, Jan. 2016, pp. 403–407.
- [8] C. Wang, M. Fan, B. Cao, B. Ye, and W. Li, "Novel noncontact eddy current measurement of electrical conductivity," *IEEE Sensors J.*, vol. 18, no. 22, pp. 9352–9359, Nov. 2018.
- [9] Z. Xia, T. Shen, Y. Su, Y. Wan, and W. Wang, "Development of a conductivity sensor as a network node for real time monitoring of water," in *Proc. IEEE 3rd Inf. Technol. Mechatronics Eng. Conf. (ITOEC)*, Chongqing, China, Oct. 2017, pp. 1092–1096.
- [10] T. P. Lambrou, C. C. Anastasiou, C. G. Panayiotou, and M. M. Polycarpou, "A low-cost sensor network for real-time monitoring and contamination detection in drinking water distribution systems," *IEEE Sensors J.*, vol. 14, no. 8, pp. 2765–2772, Aug. 2014.
- [11] N. A. Cloete, R. Malekian, and L. Nair, "Design of smart sensors for real-time water quality monitoring," *IEEE Access*, vol. 4, pp. 3900–3975, 2016.
- [12] M. Sophocleous and J. K. Atkinson, "A novel thick-film electrical conductivity sensor suitable for liquid and soil conductivity measurements," *Sens. Actuators B, Chem.*, vol. 213, pp. 417–422, Jul. 2015.
- [13] G. Liu, C. Ho, N. Slappey, Z. Zhou, S. E. Snelgrove, M. Brown, A. Grabinski, X. Guo, Y. Chen, K. Miller, J. Edwards, and T. Kaya, "A wearable conductivity sensor for wireless real-time sweat monitoring," *Sens. Actuators B, Chem.*, vol. 227, pp. 35–42, May 2016.
- [14] M. A. Yunus, S. Ibrahim, W. A. H. Altowayti, G. P. San, and S. C. Mukhopadhyay, "Selective membrane for detecting nitrate based on planar electromagnetic sensors array," in *Proc. 10th Asian Control Conf. (ASCC)*, Picataway, NJ, USA, May/Jun. 2015, pp. 1–6.
- [15] A. Azmi, A. A. Azman, K. K. Kaman, S. Ibrahim, S. C. Mukhopadhyay, S. W. Nawawi, and M. A. Yunus, "Performance of coating materials on planar electromagnetic sensing array to detect water contamination," *IEEE Sensors J.*, vol. 17, no. 16, pp. 5244–5251, Aug. 2017.
- [16] A. I. Zia, S. C. Mukhopadhyay, P.-L. Yu, I. H. Al-Bahadly, C. P. Gooneratne, and J. Kosel, "Rapid and molecular selective electrochemical sensing of phthalates in aqueous solution," *Biosensors Bioelectron.*, vol. 67, pp. 342–349, May 2015.
- [17] M. A. M. Yunus, S. C. Mukhopadhyay, and S. Ibrahim, "Planar electromagnetic sensor based estimation of nitrate contamination in water sources using independent component analysis," *IEEE Sensors J.*, vol. 12, no. 6, pp. 2024–2034, Jun. 2012.
- [18] M. E. E. Alahi, X. Li, S. Mukhopadhyay, and L. Burkitt, "Application of practical nitrate sensor based on electrochemical impedance spectroscopy," in *Sensors for Everyday Life*, S. C. Mukhopadhyay, O. A. Postolache, K. P. Jayasundera, A. K. Swain, Eds. Cham, Switzerland: Springer, 2017, pp. 109–113.
- [19] A. V. Mamishev, K. Sundara-Rajan, Y. Du, M. Zahn, and F. Yang, "Interdigital sensors and transducers," *Proc. IEEE*, vol. 95, no. 5, pp. 808–845, May 2004.
- [20] V. F. Lvovich, *Impedance Spectroscopy: Applications to Electrochemical and Dielectric Phenomena*. Hoboken, NJ, USA: Wiley, 2012, pp. 61–63.



**XIAOLEI WANG** received the Ph.D. degree in communication and information system from Wuhan University, Wuhan, China, in 2015.

He is currently a Lecturer with the Hubei Key Laboratory of Intelligent Wireless Communications, South Central University for Nationalities, Wuhan. His current research interests include novel sensor designing, sensor fusion, and environment monitoring.

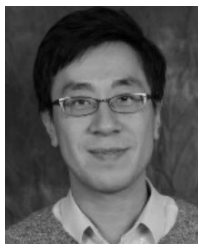


**YUHAO WANG** (SM'14) was born in Hubei, China, in 1977. He received the Ph.D. degree in space exploration technology from Wuhan University, Wuhan, China, in 2006.

In 2008, he was a Visiting Professor with the Department of Electrical Communication Engineering, University of Calgary, Calgary, AB, Canada, and with the National Mobile Communication Research Laboratory, Southeast University, Nanjing, China, from 2010 to 2011. He is currently

a Professor with the Cognition Sensor Network Laboratory, School of Information Engineering, Nanchang University, Nanchang, China. He serves for many international journals such as the *International Journal of Advanced Robotic Systems*. His current research interests include wideband wireless communication and radar sensing fusion systems, channel measurement and modeling, nonlinear signal processing, smart sensor, image and video processing, and machine learning.





**HENRY LEUNG** (F'15) received the Ph.D. degree in electrical and computer engineering from McMaster University, Hamilton, ON, Canada.

He was with the Department of National Defense of Canada, as a Defense Scientist. He is currently a Professor with the Department of Electrical and Computer Engineering, University of Calgary, Calgary, AB, Canada. His current research interests include information fusion, machine learning, the IoT, nonlinear dynamics,

robotics, signal, and image processing.

Dr. Leung is an Associate Editor of the *IEEE Circuits and Systems Magazine*. He is a Topic Editor in robotic sensors of the *International Journal of Advanced Robotic Systems*. He is an Editor of the Springer book series on *Information Fusion and Data Science*. He is a Fellow of SPIE.



**SHAOPING CHEN** received the B.S. and M.S. degrees from Wuhan University, Wuhan, China, in 1987 and 1990, respectively, all in electrical engineering, and the Ph.D. degree in information and communication engineering from the Huazhong University of Science and Technology, Wuhan, in 2004. He is currently a Professor with the Hubei Key Laboratory of Intelligent Wireless Communications, South Central University for Nationalities, Wuhan. His current research interest

includes the communications and signal processing, including transceiver design, detection and estimation, and wireless and optical communication systems.



**SUBHAS CHANDRA MUKHOPADHYAY** (F'11) received the B.E.E. (Gold Medalist), M.E.E., Ph.D. degrees in India and the D.Eng. degree in Japan.

He has over 30 years of teaching, industrial, and research experience. He was a Professor of sensing technology with Massey University, New Zealand. He is currently a Professor of mechanical/electronics engineering with Macquarie University, Australia, and the Discipline Leader of

the Mechatronics Engineering Degree Programme. He has supervised over 40 postgraduate students and over 100 Honors students. He has examined over 50 postgraduate theses. He has published over 400 articles in different international journals and conference proceedings, authored seven books and 42 book chapters, and edited 17 conference proceedings. He has also edited 32 books with SpringerVerlag and 24 journal special issues. He has delivered 328 presentations, including keynote, invited, tutorial, and special lectures. His current research interests include smart sensors and sensing technology, instrumentation techniques, wireless sensors and network (WSN), the Internet of Things (IoT), numerical field calculation, and electromagnetics.

Dr. Mukhopadhyay is a Fellow of IET, U.K., and IETE, India. He has organized over 20 international conferences as either General Chair/Co-chair or Technical Programme Chair. He chairs the IEEE IMS NSW chapter. He is a Topical Editor of the *IEEE SENSORS JOURNAL*. He is also an Associate Editor of the *IEEE TRANSACTIONS ON INSTRUMENTATION AND MEASUREMENTS*. He is a Distinguished Lecturer of the IEEE Sensors Council, from 2017 to 2019.



**YONGQIANG CUI** received the Ph.D. degree in circuit and system engineering from Wuhan University, Wuhan, China, in 2015. He is currently a Lecturer with the Hubei Key Laboratory of Intelligent Wireless Communications, South Central University for Nationalities, Wuhan. His current research interests include signal processing, the IoT, and data fusion.

...